

1 **Melatonin Attenuates Chronic Cough Mediated by Oxidative Stress**
2 **via Transient Receptor Potential Melastatin-2 in Guinea Pigs**
3 **Exposed to Particulate Matter 2.5**

4 Zhenjun Ji¹, Zhen Wang¹, Zhe Chen², Hao Jin¹, Chen Chen¹, Senlin Chai¹, Haining
5 Lv¹, Ling Yang¹, Yakun Hu¹, Rong Dong^{1*}, Kefang Lai^{2*}

6 ¹Medical School, Southeast University, Nanjing, China

7 ²State Key Laboratory of Respiratory Disease, Guangzhou Institute of Respiratory
8 Disease, The First Affiliated Hospital of Guangzhou Medical University, Guangzhou,
9 China

10 **Corresponding authors:**

11 *Kefang Lai, State Key Laboratory of Respiratory Disease, The First Affiliated
12 Hospital of Guangzhou Medical University, Guangzhou Institute of Respiratory
13 Disease, 151 Yanjiang Rd., Guangzhou, China. Email: klai@163.com.

14 *Rong Dong, Medical School of Southeast University, 87 Dingjiaqiao, Nanjing
15 210009. Email: dongrongshengli@163.com.

16 **Short Title:** Melatonin Attenuates Chronic Cough induced by PM2.5 Exposure

17 **Conflict of Interest**

18 There is no conflict of interest.

19 **Acknowledgements**

20 This work was supported by Grants 2016OP015 from Open Project of State Key
21 Laboratory of Respiratory Disease. Authors would like to thank Xinjian Zhu for his
22 assistance of experiment.

23

24 **Summary**

25 The aim of this study was to investigate the effects of melatonin on oxidative stress,
26 the expression of transient receptor potential melastatin-2 (TRPM2) in guinea pig
27 brains, and the influence of melatonin on oxidative stress in lungs and airway
28 inflammation induced by particulate matter 2.5 (PM2.5). A particle suspension (0.1
29 g/ml) was nasally administered to the guinea pigs to prepare a PM2.5 exposure model.
30 Cough frequency and cough incubation period were determined through RM6240B
31 biological signal collection and disposal system. Oxidative stress markers, including
32 malondialdehyde (MDA), total antioxidant capacity (T-AOC), total superoxide
33 dismutase (T-SOD), and glutathione peroxidase (GSH-Px), in the medulla oblongata
34 were examined through spectrophotometer. Reactive oxygen species (ROS) were
35 detected in the hypoglossal nucleus, cuneate nucleus, Botzinger complex, dorsal vagal
36 complex, and airway through dihydroethidium fluorescence. Hematoxylin-eosin (HE)
37 staining and substance P expression via immunohistochemistry revealed the
38 inflammatory levels in the airway. TRPM2 was observed in the medulla oblongata
39 through immunofluorescence and western blot. The ultrastructure of the blood–brain
40 barrier and neuronal mitochondria was determined by using a transmission electron
41 microscope. Our study suggests that melatonin treatment decreased PM2.5-induced
42 oxidative stress level in the brains and lungs and relieved airway inflammation and
43 chronic cough. TRPM2 might participate in oxidative stress in the cough center by
44 regulating cough.

45 **Key words:** melatonin, oxidative stress, cough sensitivity

46

47 **Introduction**

48 Ambient particulate matter 2.5 (PM_{2.5}) is defined as airborne particulate matter with
49 aerodynamic diameters less than 2.5µm (Chen et al. 2016). PM_{2.5} can transport
50 directly into the alveoli which is mainly derived from oil and coal combustion and
51 vehicle emissions; this pollutant is composed of elemental carbon, organic carbon,
52 aluminum, copper, nickel, sulfates, nitrates, polycyclic aromatic hydrocarbons (PAH)
53 and other compounds (WHO 2013). Air pollutants, including PM_{2.5}, are closely
54 related to respiratory symptoms and diseases, such as chronic cough, chronic
55 obstructive pulmonary diseases (COPD), asthma, and lung cancer (Falcon-Rodriguez
56 *et al.* 2016; Zhang *et al.* 2015). Chronic cough is defined as cough lasting more than
57 eight weeks without abnormal pulmonary function, and cough hypersensitivity is a
58 key pathophysiological mechanism of chronic cough (Lai *et al.* 2013). However, the
59 exact mechanism of cough hypersensitivity is unclear.

60 Cachon et al (Cachon *et al.* 2014) found that human lung epithelial cells secreted
61 more cytokines including IL-1β, IL-6 and TNF-α after exposed to PM_{2.5}. PM_{2.5}
62 could enter the blood through the alveolus–capillary barrier and penetrate the
63 blood–brain barrier (BBB) or migrate via the olfactory nerve pathway into the brain
64 and cause neuroinflammation, oxidative stress, and neuronal damage (Bos *et al.* 2014).
65 PM_{2.5}, is also related to central nervous system (CNS) diseases, such as
66 neurodegenerative diseases. Levesque et al.(Levesque *et al.* 2011) demonstrated that

67 subchronic exposure to diesel engine exhaust causes neuroinflammation and thus
68 increases the expression of α -synuclein, an early marker of neurodegenerative
69 diseases. Calderon-Garciduenas et al. (Calderon-Garciduenas *et al.* 2015a;
70 Calderon-Garciduenas *et al.* 2015b) found that neurodegenerative diseases in children
71 are triggered by exposure to particulate matters and ozone, and environmental factors
72 and gene factors promote Alzheimer's disease. Cough is a special kind of respiratory
73 activity and the medulla oblongata receives sensory signals from the cough receptors
74 in airways via vagus nerves and superior laryngeal nerves as the respiratory center.
75 The respiratory center comprises the Botzinger complex, pons respiratory group,
76 solitary nucleus group, and raphe nucleus group. These neurons in respiratory nuclei
77 which participate in the integration of the afferent cough information are thought as
78 central cough generator, and further regulate the motion of muscles in airways and
79 generate cough (Chung and Pavord 2008). Signals from periphery are also
80 subsequently transmitted into the superior center above the brainstem and it alters
81 emotion and cognition brain regions. Further studies have not yet to clarify whether
82 central nuclei generate pathological changes induced by PM2.5 and affect chronic
83 cough development.

84

85 PM2.5 stimulates the release of endogenous and exogenous free radicals, including
86 reactive oxygen species (ROS) in the CNS; as a result, the cause of
87 oxidant/antioxidant systems imbalance (Fagundes *et al.* 2015; Liu *et al.* 2015). Direct
88 PM2.5 exposure likely induces oxidative stress and neurotoxicity in the hippocampus

89 and cerebellum (Fagundes *et al.* 2015). As a multifunctional non-selective cation
90 channel with N-domain, the transient potential receptor melastatin-2 (TRPM2)
91 channel exhibits a pyrophosphatase activity, which can be activated by ROS and
92 adenosine diphosphate ribose (ADPR), and functions as a sensor for oxidative stress.
93 TRPM2 is distributed mainly in different parts of the mammalian brain, including the
94 hippocampus, cortex, thalamus, midbrain, and medulla oblongata; this channel is also
95 abundant in neurons and microglia (Naziroglu 2011; Ru and Yao 2014). High TRPM2
96 expression mediates extracellular calcium entry and induces cell death. TRPM2 is
97 also involved in many disorders, such as traumatic brain injury (Yuruker *et al.* 2015),
98 cerebral ischemia (Akpinar *et al.* 2016), type II diabetes (Sozbir and Naziroglu 2016),
99 cancers, inflammation, and neurodegenerative diseases (Naziroglu 2011). As such,
100 TRPM2 is a potentially effective target of many diseases. However, studies have not
101 yet to determine whether TRPM2 could mediate the generation of oxidative stress in
102 the respiratory center and airway, and further induce airway inflammation and cough
103 hypersensitivity.

104 Melatonin, secreted by the pineal gland, regulates the sleep, circadian rhythms and act
105 as an effective antioxidant. In various pathological states, melatonin and its
106 metabolites can function as endogenous free radical scavengers and broad-spectrum
107 antioxidants to scavenge ROS. Melatonin also elicits a neuroprotective effect and
108 protects the vascular endothelium by scavenging ROS and inhibiting
109 pro-inflammatory cytokine release and Ca²⁺ overload (Akpinar *et al.* 2016; Kahya *et*
110 *al.* 2017; Kaisar *et al.* 2015; Ma *et al.* 2015). Melatonin was hypothesized to alleviate

111 chronic cough which serve as a potential therapeutic drug for chronic cough.

112

113 This study was aimed to investigate whether melatonin could alleviate chronic cough
114 induced by PM2.5 through relieving oxidative stress and also determine whether
115 TRPM2 participates in oxidative stress in the brain and influences airway oxidative
116 stress and airway inflammation.

117

118 **Materials and Methods**

119 *Animals*

120 75 Healthy male Hartley guinea pigs (350-500g, Jiangnan Experimental Animal
121 Center) were used in this study (Figure 1). Experiments in this study were approved
122 by the Animal Care and Use Committee of the Medical School of Southeast
123 University. The animals were divided into normal saline control group, PM2.5
124 exposure group and PM2.5 exposure+melatonin treatment group. The acquisition of
125 PM2.5 and suspension preparations, and animal model preparing were similar to our
126 previous study (Lv *et al.* 2016). The PM2.5 exposure group received a 200 µl
127 suspension (0.1 g/ml) each time, nasally instilled twice a day, for 28 continuous days,
128 while the normal saline control group received equivalent saline. The PM2.5
129 exposure+melatonin treatment group received melatonin (10 mg/kg/day) via
130 intraperitoneal injection for 8 days, while PM2.5 exposure+saline treatment group
131 received equivalent saline.

132

133 ***Cough sensitivity examination***

134 Cough frequency and cough incubation period were measured by RM6240B
135 biological signal collection and disposal system (Chengdu, China). We prepared a
136 0.45 M citric acid solution. Guinea pigs were placed in a cough recorder of sound
137 energy, and the normal waveform was recorded for 10 s after the ultrasonic atomizer
138 was opened and sprayed for 15 s into the recorder. We recorded cough frequency of
139 guinea pigs within 10 min and time from the citric acid spray to the first cough of
140 animals (cough incubation periods) to assess the cough reflex sensitivity in the airway
141 of guinea pigs.

142

143 ***Tissue preparation***

144 For immunofluorescence and dihydroethidium (DHE) fluorescence, guinea pigs were
145 anesthetized by intraperitoneal injection of pentobarbital sodium (40 mg/kg), and then
146 perfused and fixed with phosphate buffer containing 4% paraformaldehyde through
147 the heart after chest opening. Then, the brain and lung tissues were placed in the fixed
148 liquid for 8 h, which were immersed in 30% sucrose solution for using after that.

149

150 ***HE staining***

151 Lung tissues were embedded in paraffin wax after fixation in 4% paraformaldehyde
152 for HE staining, and observed under light microscopy.

153

154 ***Immunofluorescence***

155 The medulla oblongata was cut into continuous coronal slices (30 μm thickness per
156 slice) from 2 mm below to 3 mm above the obex using a microtome (Leica). The
157 slices were placed in sequence into phosphate buffered solution (PBS) containing
158 0.4% Triton X-100, PBS containing 10% goat serum (Abcam), followed by
159 incubation with a rabbit polyclonal anti-TRPM2 antibody (1:200, Abcam) at 4 $^{\circ}\text{C}$
160 overnight, then rinsed in PBS for 5 min. Subsequently, the sections were incubated
161 with a goat anti-rabbit IgG/AlexaFluor 594 secondary antibody (1:400, Invitrogen) at
162 room temperature in the dark for 2 h, followed by PBS rinsing (5 min, three times),
163 then dyed by DAPI for 1 min and rinsed in PBS for 5 min. Finally, the slices were
164 sealed with glycerol for observation by fluorescence microscope. The slices were
165 observed by an Olympus fluorescence microscope (Olympus LSM-GB200, Japan)
166 and cell number analysis was performed by Image-Pro Plus (Media Cybernetics,
167 USA). Five random slices per animal were chosen for counting at a higher
168 magnification (200 \times). The average number of five slices represented the value per
169 animal.

170

171 ***Immunohistochemistry***

172 Lung tissue (size of 0.8 cm \times 0.6 cm \times 0.2 cm) was cut into continuous coronal slices
173 (45 μm thickness per slice). Briefly, the slices were placed in deionized water
174 containing 3% H_2O_2 , rinsed in PBS (5 min, three times), incubated in rabbit serum
175 (Abcam) at room temperature for 4 h, followed by incubation with goat anti-SP
176 polyclonal antibody (1:200, Santa Cruz) at 4 $^{\circ}\text{C}$ overnight, then rinsed in PBS for 5

177 min. The slices were sequentially incubated with biotinylated rabbit anti-goat IgG
178 (Boster) for 2 h, rinsed in PBS (5 min, three times), incubated with SABC (Boster) for
179 1 h, and followed by PBS rinsing (5 min, three times). The slices were stained with
180 DAB (ZSGB-BIO) and dehydrated using graded ethanol and dimethylbenzene. The
181 slices were sealed with a neutral resin under a microscope. Image-Pro Plus was used
182 to calculate mean optical density (MOD) of SP in the lungs. The five random slices
183 per animal were chosen for calculation and the mean data of five slices represented
184 the value per animal.

185

186 *DHE fluorescence*

187 Tissues were prepared as discussed above. The slices were sequentially placed into
188 PBS containing 0.4% Triton X-100, followed by incubation with 2 μ M DHE working
189 solution at 37 °C for 40 min in the dark, and rinsing with PBS (5 min, three times).
190 Finally, the slices were sealed with glycerol for observation by fluorescence
191 microscope. Cell counting and fluorescence intensity were performed as described
192 above.

193

194 *Measurement of peroxide and antioxidant enzymes*

195 The guinea pigs were decapitated directly and the medulla oblongata was rapidly
196 stripped. Tissues were mechanically homogenized and mixed with saline using a ratio
197 of weight (g): volume (ml)=1:9 under an ice-water bath. The homogenates were
198 centrifuged at 2500 rpm for 10 min. Furthermore, protein content of supernatant was

199 measured by a 720 spectrophotometer. All procedures referred to the specifications of
200 malondialdehyde (MDA)/total antioxidant capacity (T-AOC)/total superoxide
201 dismutase (T-SOD)/glutathione peroxidase (GSH-Px) kits (Jiancheng, Nanjing,
202 China).

203

204 ***Western blot***

205 The medulla oblongata tissues of guinea pigs were homogenized in a lysis buffer
206 (Beyotime, China) and were then centrifuged at 12,000 rpm for 20 min. Then, the
207 samples were placed in 12% acrylamide denaturing gels (SDS-PAGE) and transferred
208 to nitrocellulose membranes (Sigma) after electrophoresis, followed by incubation for
209 1 h at room temperature with 5% non-fat dry milk in Tris Buffered Saline Tween
210 (TBST). Then, the membranes were sequentially incubated with rabbit anti-TRPM2
211 (1:2000, Abcam, USA) and HRP-linked goat anti-rabbit antibody (1:5000, Invitrogen).
212 Signals were captured by Microchemi chemiluminescent image analysis system
213 (DNR Bio-imaging Systems, Jerusalem, Israel) after handling with the enhanced
214 chemiluminescence method. Blots were quantified by Image-Pro Plus.

215

216 ***Transmission electron microscopy***

217 Guinea pigs were anesthetized with 10% chloral hydrate (3 ml/kg to 4 mL/kg, ip) and
218 perfused with normal saline, followed by phosphate buffer containing 4%
219 paraformaldehyde and 0.5% glutaraldehyde (Sigma). Tissues in dorsal vagal complex
220 (DVC) were diced and fixed in 2.5% chilled glutaraldehyde. A 1 mm³ tissue block

221 was post-stained with uranyl acetate and lead citrate. Tissue sections were cut to
222 50-nm thicknesses and observed under a transmission electron microscope (JEOL,
223 JEM-1010, Japan).

224

225 *Statistical analysis*

226 All data are analyzed by SPSS 19.0 and presented as the means \pm S.E.M. An
227 independent-samples T-test was used to compare between two groups. Values of
228 $p < 0.05$ were considered statistically significant.

229

230 **Results**

231 *Cough sensitivity examination*

232 The cough frequency of the saline group, PM2.5 exposure group, and PM2.5
233 exposure+melatonin treatment groups were 8.46 ± 1.02 , 25.92 ± 2.74 , 18.77 ± 1.77 ,
234 respectively, while the cough incubation periods were 68.46 ± 8.38 , 35.69 ± 6.17 ,
235 57.77 ± 7.26 . Compared with the saline group, the PM2.5 exposure group showed
236 increased cough frequency ($p < 0.001$) and decreased cough incubation period
237 ($p < 0.01$). After melatonin treatment, the PM2.5 exposure+melatonin treatment group
238 showed decreased cough frequency ($p < 0.05$) and increased cough incubation period
239 ($p < 0.05$) (Fig 2). The results indicated that PM2.5 exposure increased cough
240 sensitivity which was prevented by melatonin.

241

242 *Airway neurogenic inflammation and oxidative stress*

243 HE staining showed mucosa edema of the trachea and inflammatory cells infiltration,
244 such as increased neutrophils, monocytes, lymphocytes and eosinophils, indicating
245 exacerbated airway inflammation, which was relieved after melatonin treatment (Fig.
246 3A). Immunoreactive substances of airway neurogenic inflammatory mediator
247 substance P were dyed brown granules with cytoplasm staining and were mainly
248 distributed around the airway. The MOD of substance P in the saline group, PM2.5
249 exposure group, and PM2.5 exposure+melatonin group were 0.19 ± 0.03 , 0.42 ± 0.05 ,
250 0.21 ± 0.04 , respectively. Compared with that in the saline group, the substance P
251 expression increased after PM2.5 exposure ($p<0.01$), while substance P expression
252 decreased after melatonin treatment ($p<0.05$) (Fig. 3B 3D). These results
253 demonstrated that PM2.5 induced airway inflammation and melatonin had an
254 antagonistic effect towards inflammation. DHE fluorescence of airway showed that
255 fluorescence intensity of airway in PM2.5 exposure group is higher than that of the
256 control group, which were decreased by melatonin ($p<0.05$) (Fig. 3C 3E). The MOD
257 of ROS in the saline group, PM2.5 exposure group, and PM2.5 exposure+melatonin
258 group were 0.05 ± 0.00 , 0.06 ± 0.02 , 0.05 ± 0.02 , respectively. These results indicate that
259 PM2.5 exposure elevates the level of oxidative stress in the airway of guinea pigs,
260 which were decreased by melatonin.

261

262 ***Injury of BBB and neurons***

263 The ultrastructure in the DVC observed by transmission electron microscope showed
264 normal microvascular endothelium, astrocytes, and mitochondria structure with

265 double membrane, and parallel arrangement of mitochondrial cristae in control group.
266 The PM2.5 exposure group showed isolated microvascular endothelium, mild edema
267 of astrocytes, and narrow vessels, which indicated injury of BBB. Besides,
268 mitochondria were swollen and vacuolate, and were in disarray, with a decreased
269 number of mitochondria and mitochondrial cristae. Essentially, damage to the BBB
270 and mitochondria was relieved after intervention of melatonin (Fig. 4).

271

272 *Oxidative stress in medulla oblongata*

273 MDA represented the level of free radicals as lipid peroxides, while levels of
274 T-AOC/T-SOD/GSH-Px represented the ability of scavenging free radical as
275 antioxidant enzymes. Compared with the saline group, the PM2.5 exposure group
276 showed increased levels of MDA representing the level of oxidation and decreased
277 levels of T-AOC/GSH-Px representing antioxidant levels. However, decrease of
278 T-SOD was not obvious significantly ($p<0.1$). PM2.5 exposure+melatonin group
279 showed obviously decreased level of MDA and increased levels of
280 T-AOC/T-SOD/GSH-Px (Fig 5A).

281 DHE marks the cytoplasm and nuclei of dead neurons producing ROS red (excitation
282 535 nm, emission 610 nm). Compared with the saline group, the PM2.5 exposure
283 group showed an increased production of ROS in the hypoglossal nucleus, cuneate
284 nucleus, Botzinger complex, and DVC ($p<0.05$). Meanwhile, ROS production in
285 PM2.5 exposure+melatonin group was decreased in relevant nuclei ($p<0.05$). Our
286 data showed that PM2.5 exposure induced oxidative stress in the medulla oblongata

287 and melatonin treatment decreased the generation of ROS (Fig. 5B 5C).

288

289 ***TRPM2 expression in medulla oblongata***

290 The cytoplasm of immunoreactive neurons of TRPM2 were stained red under a
291 fluorescence microscope. Compared with the saline group, the PM2.5 exposure group
292 showed an increased expression of TRPM2 in the DVC and Botzinger complex
293 ($p<0.01$). Melatonin treatment decreased the expression of TRPM2 ($p<0.05$) (Fig. 6A
294 6B). Western blot showed that the protein level of TRPM2 in PM2.5 exposure group
295 was higher than the saline and melatonin groups ($p<0.05$) (Fig. 6C 6D).

296

297 **Discussion**

298 In our study, the particles were collected from five urban areas, including commercial
299 areas, business areas, busy traffic intersections, industrial districts, and suburbs (Lv *et*
300 *al.* 2016), and were mixed to represent the actual constituents of environmental
301 PM2.5.

302

303 The increased cough sensitivity of guinea pigs after PM2.5 exposure showed that
304 PM2.5 elicited chronic cough. We also found that PM2.5 exposure promoted the
305 infiltration of inflammatory cells, including neutrophils, monocytes, lymphocytes, and
306 eosinophils. Substance P expression was also increased which consequently induced
307 the neurogenic inflammation in the airway; as a result, cause of airway inflammation
308 which was consistent with the inflammatory phenomena of gastroesophageal reflux

309 cough (GERC), cough variant cough (CVA) and chronic cough with definite etiology.
310 Generally, guinea pigs after PM2.5 exposure showed cough hypersensitivity and the
311 same pathological characteristics as chronic cough with definite etiology, which
312 demonstrated that PM2.5 induced chronic cough. Airway neurogenic inflammation
313 was induced by neuropeptides or neurotransmitters released by airway sensory nerve
314 terminal, characterized by increased vascular permeability, plasma extravasation, and
315 tissue edema. Substance P, Calcitonin Gene-Related Peptide (CGRP), and other
316 substances stimulate vasodilation, plasma leakage, and mucus secretion, increase
317 cough sensitivity, and trigger chronic cough. We further demonstrated that PM2.5
318 could increase oxidative stress levels, which could enhance the expression of
319 inflammatory factors, such as interleukin (IL), via the NF-KB pathway and
320 accumulate inflammatory cells. Airway inflammation and oxidative stress are two
321 possible mechanisms exacerbating chronic cough, and ROS and inflammation are
322 closely associated.

323

324 Cough is a special respiratory activity and respiratory defensive reflex. The
325 respiratory center is located mostly in the medulla oblongata of brainstem, comprising
326 the dorsal respiratory group with the solitary nucleus, and the ventral respiratory
327 group containing the Botzinger complex. The stimuli of cough receptors including
328 slowly and rapidly adapting stretch receptors (SAR and RAR) and C-fiber in the
329 airway, are transmitted to the solitary nucleus via the glossopharyngeal and vagus
330 nerves to regulate the basic rhythm of inhalation. The DVC is composed of the dorsal

331 nucleus of the vagus nerve (DMV), the nucleus of the solitary tract (NTS), and the
332 area postrema. The DMV, hypoglossal nucleus, and nucleus ambiguus receive afferent
333 fibers from the NTS (Kubin *et al.* 2006). The neuronal axons of the Botzinger
334 complex projections are extensive in various regions of the medulla oblongata and
335 spinal cord associated with breathing, and these axons inhibit the discharge of
336 inhalation neurons during the expiratory phase to participate in maintaining the
337 expiratory phase. Therefore, the mutual association between the central nervous
338 system and airway has the neuroanatomical foundation. Afferent stimuli in the airway
339 can reach the cough center in the brainstem including the DVC and the ventral
340 Botzinger complex in the medulla oblongata through the sensory afferent nerve. The
341 cough center also regulates respiratory and throat muscles after signals are integrated
342 and further generates cough (Mazzone. and Udem. 2017).

343

344 BBB consists of vascular endothelial cell, tight junction between endothelium,
345 astrocyte, pericyte and basement membrane. In the ultrastructure observed with a
346 transmission electron microscope, isolated microvascular endothelium, mild edema of
347 astrocytes, and narrow vessels were present, and this observation indicated that PM2.5
348 could damage the BBB. Fang et al. (Liu *et al.* 2015) found that PM2.5 disrupts the
349 tight junction of endothelial cells, increases penetrability, and enhances monocyte
350 migration ability and demonstrated that PM2.5 can reach the CNS through the BBB;
351 the neurotoxicity of PM2.5 is also mediated by glutamate. Swollen and vacuolate
352 mitochondria were also observed in the ultrastructure, and the number of the

353 mitochondria and mitochondrial cristae was decreased. These findings suggested that
354 PM2.5 induced mitochondrial injury, which could trigger imbalance in calcium
355 homeostasis and energy metabolism in cells, and neuronal injury or apoptosis. The
356 leakage of the mitochondrial electron transport chain is also a vital source of
357 intracellular ROS, leading to oxidant/antioxidant imbalance (Redza-Dutordoir and
358 Averill-Bates 2016). We also found that the MDA level was increased, whereas
359 T-SOD, GSH-Px, and T-AOC levels were decreased after PM2.5 exposure. DHE
360 fluorescence demonstrated that ROS production was increased in DVC, Botzinger
361 complex, hypoglossal nucleus, and cuneate nucleus. These observations showed that
362 the medulla oblongata was in a state of high oxidative stress after PM2.5 exposure. It
363 was reported that cerebral ischemia, epilepsy, and trauma result in the generation of
364 oxidative stress (Halliwell 2006), which was related to BBB endothelial damage and
365 was relieved by antioxidants (Kaisar *et al.* 2015). Oxidative stress is also relevant to
366 neurodegenerative diseases. Children exposed to air pollutants, including PM2.5, in
367 Mexico City Metropolitan Area manifest signs and symptoms of early oxidative stress,
368 inflammation, innate and adaptive immunity-related genes, and BBB disruption,
369 resulting in the early neurodegenerative changes in children (Calderon-Garciduenas *et*
370 *al.* 2015b). Hence, during the process of air pollutants inducing chronic cough, the
371 activity of the cough reflex is strengthened, and oxidative stress in the center is
372 enhanced as the generation of airway inflammation. Further, the cough center is
373 remodeled, and chronic cough generated.

374

375 TRPM2 is a cation channel that exhibits oxidative stress sensitivity and mediates
376 oxidative stress-induced cell death via Ca^{2+} overload (Ru and Yao 2014). Our
377 immunofluorescence results revealed that PM2.5 exposure increased the TRPM2
378 expression in respiratory nuclei, Botzinger complex, and DVC, whereas oxidative
379 stress levels were increased. These findings were also confirmed through western blot.
380 The TRPM2 channel consists of six transmembrane segments with a pore-forming
381 loop between segments 5 and 6. The N-terminal of TRPM2 contains an IQ-like
382 calmodulin-binding motif and the C-terminal comprises a Nudix-like domain, which
383 can be bound by ADPR. Calcium overload after TRPM2 activation in microglia and
384 astrocytes can lead to mitochondrial dysfunction, and calcium overload is also related
385 to synaptic plasticity change and dementia (Wang *et al.* 2016a). TRPM2-mediated
386 Ca^{2+} influx activated by oxidative stress inhibits autophagy (Wang *et al.* 2016b).

387

388 We utilized antioxidant melatonin to elucidate the role of ROS and TRPM2 in the
389 guinea pig model of PM2.5 exposure. Melatonin treatment decreased the oxidative
390 stress level in the medulla oblongata, the TRPM2 expression in the Botzinger
391 complex and DVC. These findings indicated that ROS might be involved in TRPM2
392 activation. Vehbi Yürüker *et al.* (Yuruker *et al.* 2015) also found that melatonin
393 alleviates oxidative stress and apoptosis by inhibiting Ca^{2+} and TRPM2 channels in
394 the hippocampus of rats with traumatic brain injury; this observation suggests that
395 melatonin exhibits neuroprotective activity. The GSH-Px levels changed most
396 obviously possibly because melatonin maintains the glutathione balance by

397 stimulating the generation of glutathione peroxidase, glutathione reductase, and
398 glucose-6-phosphate dehydrogenase (Reiter *et al.* 2000). Hence, melatonin could
399 upregulate the levels of T-SOD/GSH-Px/glutathione reductase by eliciting an indirect
400 antioxidant effect and by directly scavenging free radicals and reducing MDA
401 production. Mehmet Cemal *et al.* (Kahya *et al.* 2017) demonstrated that melatonin
402 and selenium can prevent the apoptosis of neurons in the hippocampus and dorsal root
403 ganglion of diabetic rats by reducing ROS and calcium influx associated with TRPM2
404 and TRPV1. Melatonin can also function at the genetic level to prevent DNA
405 degradation and activate DNA repair enzyme. Melatonin binding sites are also found
406 in cell nuclei. Melatonin metabolites, namely,
407 *N*-1-acetyl-*N*-2-formyl-5-methoxykynuramine and *N*-1-acetyl-5-methoxykynuramine,
408 induce a similar antioxidant effect to melatonin. Transmission electron microscopy
409 revealed that melatonin relieved the injuries of BBB and mitochondria in the DVC.
410 The melatonin transporter located on the mitochondrial outer membrane and
411 melatonin can be secreted by mitochondria and induce an agglomeration effect. The
412 concentration of melatonin in the mitochondria is higher than that in other organelles.
413 Melatonin can inhibit the mitochondrial permeability transition pore (MPTP) in the
414 mitochondrial membrane and activate uncoupling proteins (UCPs). The inhibition of
415 MPTP can maintain the mitochondrial membrane potential ($\Delta \Psi$), which can
416 reduced by UCPs; thus, electron transfer can be accelerated, the efficiency of the
417 mitochondrial electron transport chain can be improved, and electron leakage and
418 ROS production can be reduced. Moreover, melatonin can prevent neuronal apoptosis

419 by decreasing the levels of pro-apoptotic factors and by activating JAK2/STAT3 and
420 BCL2 pathways (Ganie *et al.* 2016; Tan *et al.* 2016). The antioxidant edaravone can
421 also alleviate brain injuries of acute CO poisoning rats (Li *et al.* 2016). In cerebral
422 ischemia rat models, dexmedetomidine generates a neuroprotective effect by reducing
423 oxidative stress and inhibiting Ca²⁺ entry and apoptosis (Akpınar *et al.* 2016). Our
424 experiment showed a decrease in cough sensitivity and reduced substance P
425 expression and inflammation and oxidative stress levels in the airway after melatonin
426 treatment. Therefore, melatonin could alleviate chronic cough induced by PM2.5 to
427 some extent. Melatonin also shows an efficient anti-inflammation ability in airway
428 hyper-reactivity (Chen *et al.* 2011), acute lung injury (Zhang *et al.* 2016), and
429 neurogenic pulmonary edema (Chen *et al.* 2015) in rat or mouse models.

430

431 Our study demonstrated airway-generated inflammation, oxidative stress, and cough
432 hypersensitivity in guinea pigs exposed to PM2.5. The cough center also showed high
433 levels of oxidative stress and TRPM2, and injury of BBB and mitochondrial, but these
434 conditions were alleviated by melatonin treatment. Therefore, TRPM2 might be
435 involved in oxidative stress in the brain and regulation of peripheral inflammation by
436 increasing calcium influx and neuronal apoptosis.

437

438 In conclusion, our findings mainly suggested that melatonin treatment could relieve
439 cough by decreasing the expression of TRPM2 in the cough center, alleviating
440 oxidative stress in the brain or airway, and relieving airway inflammation. However,

441 the exact role of TRPM2 in the brain region that regulates airway oxidative stress and
442 inflammation should be further investigated on the basis of antagonist intervention or
443 TRPM2 knockout mice.

444 **References**

- 445 AKPINAR H, NAZIROGLU M, OVEY IS, CIG B, AKPINAR O: The neuroprotective action of
446 dexmedetomidine on apoptosis, calcium entry and oxidative stress in cerebral
447 ischemia-induced rats: Contribution of TRPM2 and TRPV1 channels. *Sci. Rep.* **6**: 37196,
448 2016.
- 449 BOS I, DE BOEVER P, INT PANIS L, MEEUSEN R: Physical activity, air pollution and the brain.
450 *Sports Med.* **44**: 1505-18, 2014.
- 451 CACHON BF, FIRMIN S, VERDIN A, AYI-FANOUE L, BILLET S, CAZIER F, MARTIN PJ, AISSI F,
452 COURCOT D, SANNA A, SHIRALI P: Proinflammatory effects and oxidative stress within
453 human bronchial epithelial cells exposed to atmospheric particulate matter (PM(2.5) and
454 PM(>2.5)) collected from Cotonou, Benin. *Environ. Pollut.* **185**: 340-51, 2014.
- 455 CALDERON-GARCIDUENAS L, MORA-TISCARENO A, MELO-SANCHEZ G,
456 RODRIGUEZ-DIAZ J, TORRES-JARDON R, STYNER M, MUKHERJEE PS, LIN W,
457 JEWELLS V: A Critical Proton MR Spectroscopy Marker of Alzheimer's Disease Early
458 Neurodegenerative Change: Low Hippocampal NAA/Cr Ratio Impacts APOE varepsilon4
459 Mexico City Children and Their Parents. *J. Alzheimers Dis.* **48**: 1065-75, 2015a.
- 460 CALDERON-GARCIDUENAS L, VOJDANI A, BLAUROCK-BUSCH E, BUSCH Y, FRIEDLE A,
461 FRANCO-LIRA M, SARATHI-MUKHERJEE P, MARTINEZ-AGUIRRE X, PARK SB,
462 TORRES-JARDON R, D'ANGIULLI A: Air pollution and children: neural and tight junction
463 antibodies and combustion metals, the role of barrier breakdown and brain immunity in
464 neurodegeneration. *J. Alzheimers Dis.* **43**: 1039-58, 2015b.
- 465 CHEN CF, WANG D, REITER RJ, YAN LE J: Oral melatonin attenuates lung inflammation and
466 airway hyperreactivity induced by inhalation of aerosolized pancreatic fluid in rats. *J. Pineal*
467 *Res.* **50**: 46-53, 2011.
- 468 CHEN JY, QIAN C, DUAN HY, CAO SL, YU XB, LI JR, GU C, YAN F, WANG L, CHEN G:
469 Melatonin attenuates neurogenic pulmonary edema via the regulation of inflammation and
470 apoptosis after subarachnoid hemorrhage in rats. *J. Pineal Res.* **59**: 469-477, 2015.
- 471 CHEN R, HU B, LIU Y, XU J, YANG G, XU D, CHEN C: Beyond PM2.5: The role of ultrafine
472 particles on adverse health effects of air pollution. *Biochim. Biophys. Acta.* **1860**: 2844-55,
473 2016.
- 474 CHUNG KF, PAVORD ID: Prevalence, pathogenesis, and causes of chronic cough. *The Lancet.* **371**:
475 1364-1374, 2008.
- 476 FAGUNDES LS, FLECK ADA S, ZANCHI AC, SALDIVA PH, RHODEN CR: Direct contact with
477 particulate matter increases oxidative stress in different brain structures. *Inhal. Toxicol.* **27**:
478 462-7, 2015.
- 479 FALCON-RODRIGUEZ CI, OSORNIO-VARGAS AR, SADA-OVALLE I, SEGURA-MEDINA P:
480 Aeroparticles, Composition, and Lung Diseases. *Front. Immunol.* **7**: 3, 2016.

481 GANIE SA, DAR TA, BHAT AH, DAR KB, ANEES S, ZARGAR MA, MASOOD A: Melatonin: A
482 Potential Anti-Oxidant Therapeutic Agent for Mitochondrial Dysfunctions and Related
483 Disorders. *Rejuvenation Res.* **19**: 21-40, 2016.

484 HALLIWELL B: Oxidative stress and neurodegeneration: where are we now? *J. Neurochem.* **97**:
485 1634-58, 2006.

486 KAHYA MC, NAZIROGLU M, OVEY IS: Modulation of Diabetes-Induced Oxidative Stress,
487 Apoptosis, and Ca²⁺ Entry Through TRPM2 and TRPV1 Channels in Dorsal Root Ganglion
488 and Hippocampus of Diabetic Rats by Melatonin and Selenium. *Mol. Neurobiol.* **54**:
489 2345-2360, 2017.

490 KAISAR MA, PRASAD S, CUCULLO L: Protecting the BBB endothelium against cigarette
491 smoke-induced oxidative stress using popular antioxidants: Are they really beneficial? *Brain*
492 *Res.* **1627**: 90-100, 2015.

493 KUBIN L, ALHEID GF, ZUPERKU EJ, MCCRIMMON DR: Central pathways of pulmonary and
494 lower airway vagal afferents. *J Appl Physiol (1985)*. **101**: 618-27, 2006.

495 LAI KF, CHEN RC, ZHONG NS: Air Pollution and Chronic Cough in China Response. *Chest.* **144**:
496 363-364, 2013.

497 LEVESQUE S, SURACE MJ, MCDONALD J, BLOCK ML: Air pollution & the brain: Subchronic
498 diesel exhaust exposure causes neuroinflammation and elevates early markers of
499 neurodegenerative disease. *J. Neuroinflammation.* **8**: 105, 2011.

500 LI Q, BI MJ, BI WK, KANG H, YAN LE J, GUO YL: Edaravone attenuates brain damage in rats after
501 acute CO poisoning through inhibiting apoptosis and oxidative stress. *Environ. Toxicol.* **31**:
502 372-9, 2016.

503 LIU F, HUANG Y, ZHANG F, CHEN Q, WU B, RUI W, ZHENG JC, DING W: Macrophages treated
504 with particulate matter PM_{2.5} induce selective neurotoxicity through glutaminase-mediated
505 glutamate generation. *J. Neurochem.* **134**: 315-26, 2015.

506 LV H, YUE J, CHEN Z, CHAI S, CAO X, ZHAN J, JI Z, ZHANG H, DONG R, LAI K: Effect of
507 transient receptor potential vanilloid-1 on cough hypersensitivity induced by particulate matter
508 2.5. *Life Sci.* **151**: 157-66, 2016.

509 MA P, LIU X, WU J, YAN B, ZHANG Y, LU Y, WU Y, LIU C, GUO J, NANBERG E, BORNEHAG
510 CG, YANG X: Cognitive deficits and anxiety induced by diisononyl phthalate in mice and the
511 neuroprotective effects of melatonin. *Sci. Rep.* **5**: 14676, 2015.

512 MAZZONE. SB, UNDEM. BJ: Vagal afferent innervation of the airways in health and disease. *Physiol.*
513 *Rev.* **96**: 975-1024, 2017.

514 NAZIROGLU M: TRPM2 cation channels, oxidative stress and neurological diseases: where are we
515 now? *Neurochem. Res.* **36**: 355-66, 2011.

516 REDZA-DUTORDOIR M, AVERILL-BATES DA: Activation of apoptosis signalling pathways by
517 reactive oxygen species. *Biochim. Biophys. Acta.* **1863**: 2977-2992, 2016.

518 REITER RJ, TAN DX, OSUNA C, GITTO E: Actions of Melatonin in the Reduction of Oxidative
519 Stress. *J. Biomed. Sci.* **7**: 444-458, 2000.

520 RU XC, YAO XQ: TRPM2: a multifunctional ion channel for oxidative stress sensing. *Acta*
521 *Physiologica Sinica.* **66**: 7-15, 2014.

522 SOZBIR E, NAZIROGLU M: Diabetes enhances oxidative stress-induced TRPM2 channel activity and
523 its control by N-acetylcysteine in rat dorsal root ganglion and brain. *Metab. Brain Dis.* **31**:
524 385-93, 2016.

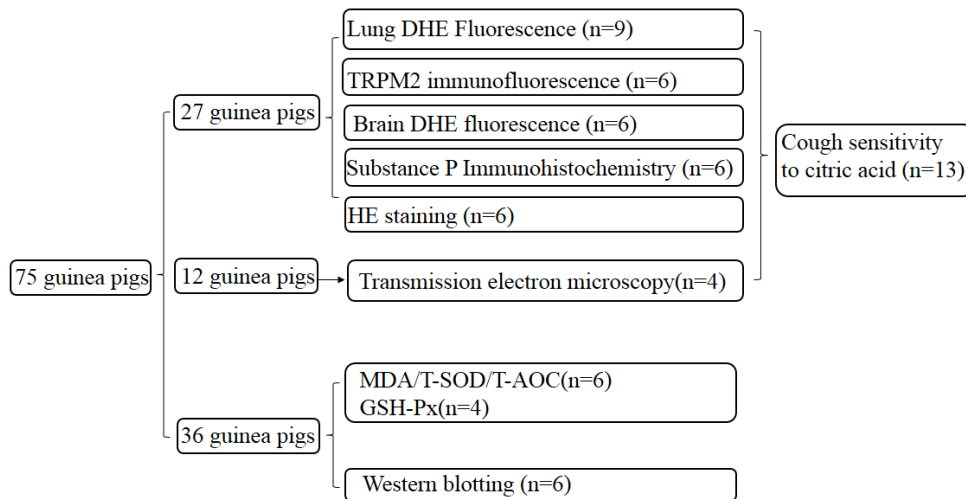
525 TAN DX, MANCHESTER LC, QIN L, REITER RJ: Melatonin: A Mitochondrial Targeting Molecule
526 Involving Mitochondrial Protection and Dynamics. *Int J Mol Sci.* **17**, 2016.
527 WANG J, JACKSON MF, XIE YF: Glia and TRPM2 Channels in Plasticity of Central Nervous System
528 and Alzheimer's Diseases. *Neural Plast.* **2016**: 1680905, 2016a.
529 WANG Q, GUO WJ, HAO BX, SHI XL, LU YY, WONG CWM, MA VWS, YIP TTC, AU JSK, HAO
530 Q, CHEUNG KH, WU WT, LI GR, YUE JB: Mechanistic study of
531 TRPM2-Ca²⁺-CAMK2-BECN1 signaling in oxidative stress-induced autophagy inhibition.
532 *Autophagy.* **12**: 1340-1354, 2016b.
533 WHO: Health Effects of Particulate Matter. Policy implications for countries in eastern Europe,
534 Caucasus and central Asia. *Copenhagen: WHO Regional Office for Europe.* 2013.
535 YURUKER V, NAZIROGLU M, SENOL N: Reduction in traumatic brain injury-induced oxidative
536 stress, apoptosis, and calcium entry in rat hippocampus by melatonin: Possible involvement of
537 TRPM2 channels. *Metab. Brain Dis.* **30**: 223-31, 2015.
538 ZHANG Q, QIU M, LAI K, ZHONG N: Cough and environmental air pollution in China. *Pulm.*
539 *Pharmacol. Ther.* **35**: 132-6, 2015.
540 ZHANG Y, LI XR, CRAILLER JJ, WANG N, WANG MM, YAO JF, ZHONG R, GAO GF, WARD
541 PA, TAN DX, LI XD: Melatonin alleviates acute lung injury through inhibiting the NLRP3
542 inflammasome. *J. Pineal Res.* **60**: 405-414, 2016.

543

544 **Figure legends**

545 Fig 1.

546 The distribution of guinea pigs in various groups are shown in the figure. There are in
547 total 75 guinea pigs in our study. All guinea pigs were randomly divided into 3 groups
548 including normal saline control group, PM2.5 exposure group and PM2.5
549 exposure+melatonin treatment group. According to different handling methods, 27
550 guinea pigs were used for examination of DHE fluorescence, TRPM2
551 immunofluorescence, SP immunohistochemistry, and HE staining. 36 guinea pigs
552 were used for western blotting and examination of MDA/T-SOD/T-AOC/GSH-Px.
553 Another 12 guinea pigs were used for observation by transmission electron
554 microscopy.



555

556

557 Fig 2.

558 Values for cough sensitivity examination. (A) Cough frequency showed significant

559 differences between saline control group and PM2.5 exposure group, so was that

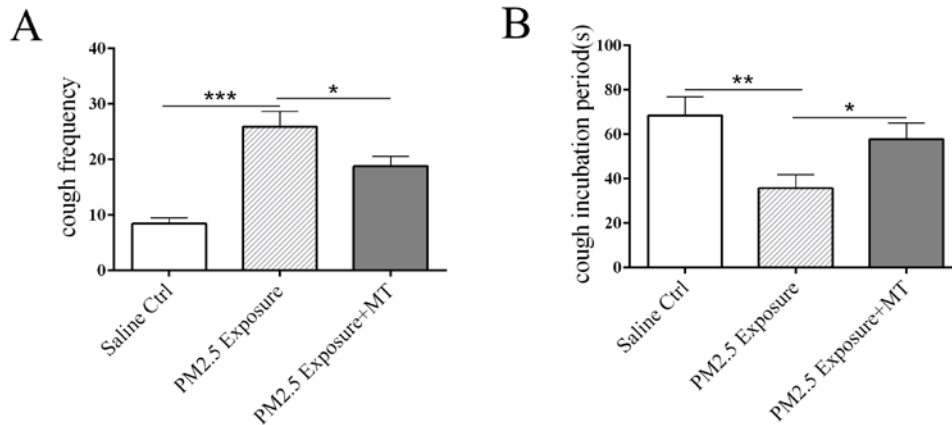
560 between PM2.5 exposure group and PM2.5 exposure+melatonin group. (B) Cough

561 incubation period of PM2.5 exposure group was less than saline control group, while

562 PM2.5 exposure+melatonin group had prolonged period than PM2.5 exposure group.

563 The values are presented as the means \pm S.E.M. * $p < 0.05$, ** $p < 0.01$, and *** $p < 0.001$,

564 independent-samples T-test. n=13 per group.



565

566

567 Fig 3.

568 Airway inflammation and oxidative stress in guinea pigs. (A) HE staining showing

569 the pathological changes in lungs. (B) Representative images of substance P

570 immunostaining. (C) Representative images of DHE fluorescence in airway. (D) The

571 bar graph representing quantified results of substance P. Compared with that in the

572 saline group, the substance P expression increased after PM2.5 exposure ($p < 0.01$),

573 while substance P expression decreased after melatonin treatment ($p < 0.05$). (E) The

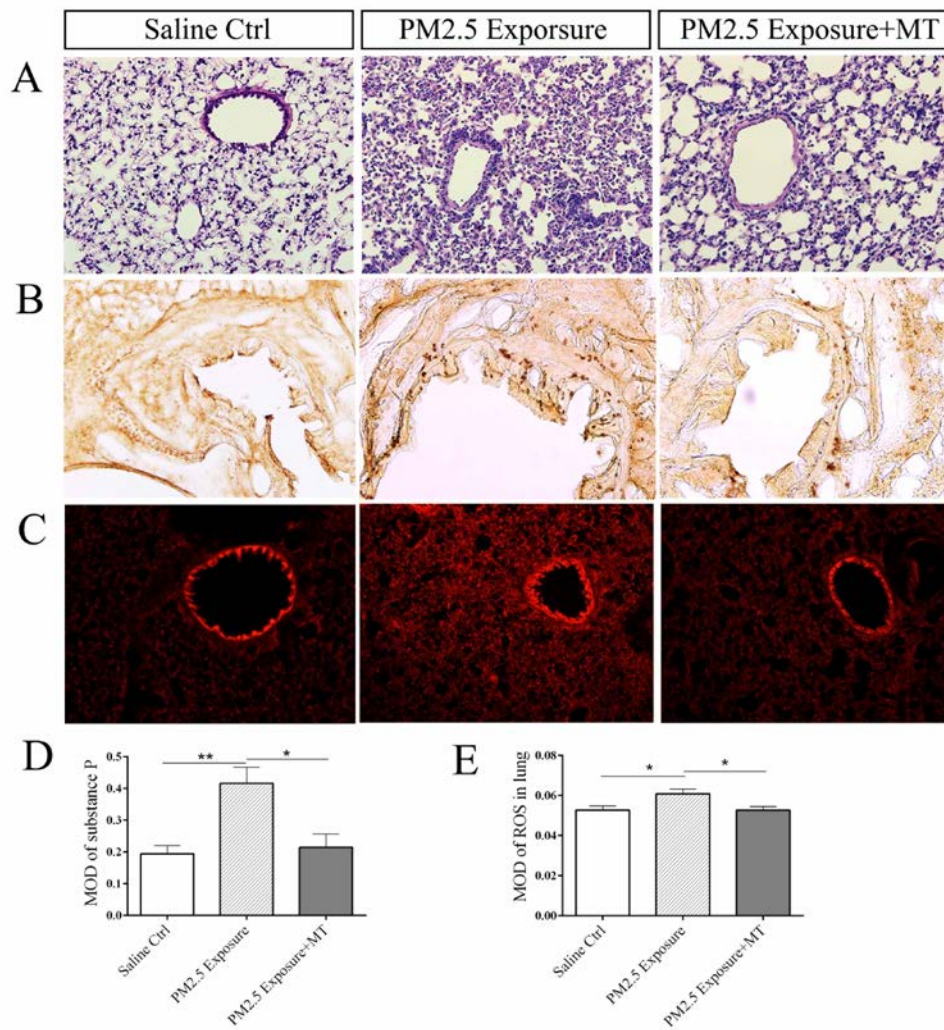
574 bar graph representing quantified results of lung ROS. Compared with that in the

575 saline group, the MOD of ROS increased after PM2.5 exposure ($p < 0.05$), while the

576 MOD values decreased after melatonin treatment ($p < 0.05$). The values are presented

577 as the means \pm S.E.M. * $p < 0.05$, ** $p < 0.01$, independent-samples T-test. n=6-9 per

578 group. $\times 200$



579

580

581 Fig 4.

582 Ultramicroscopic images of BBB and mitochondria in dorsal vagal complex taken by

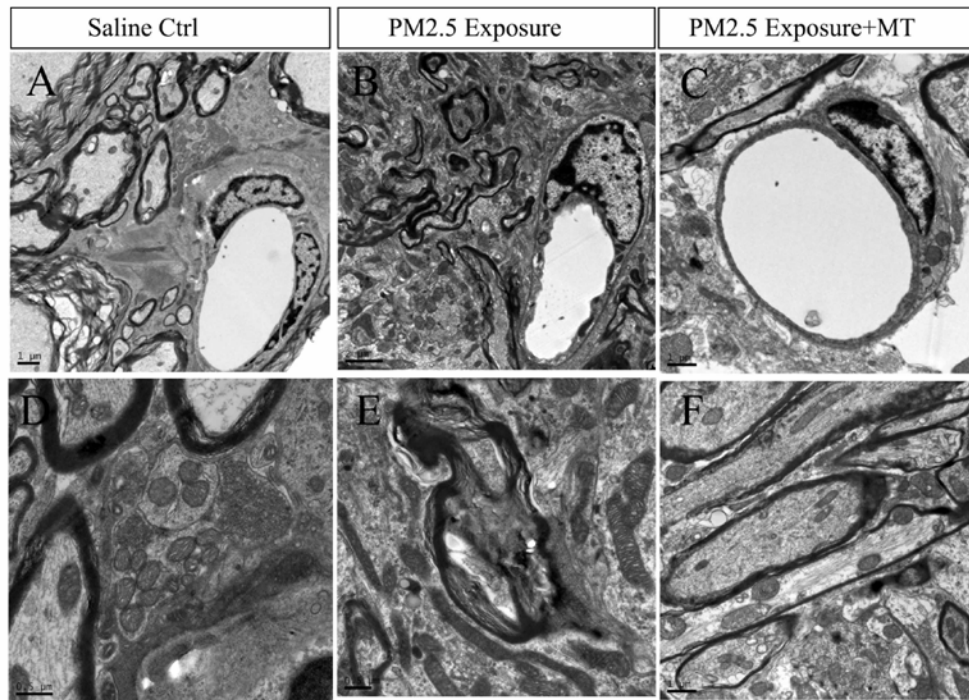
583 transmission electron microscope. (A-C) Representative images of BBB in the saline

584 control group, PM2.5 exposure group, and PM2.5 exposure group+melatonin

585 treatment group. (D-F) Representative mitochondrial ultrastructure in three groups.

586 Scale bar = 0.5 μ m in figure D and E, and Scale bar = 1 μ m in figure A, C, and F, and

587 2 μ m in figure B.



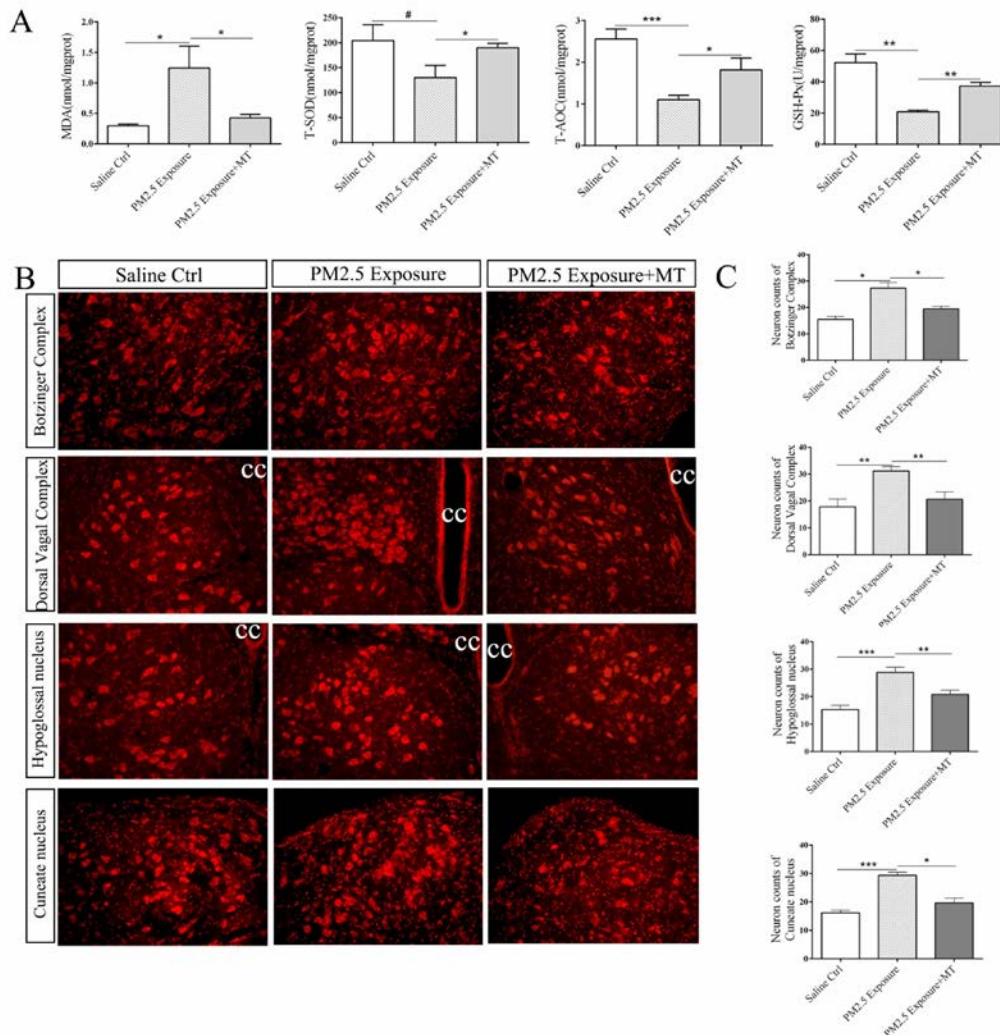
588

589

590 Fig 5.

591 Levels of oxidative stress of medulla oblongata. (A) Levels of MDA/T-SOD/T-AOC
592 and GSH-Px in medulla oblongata of saline control group, PM2.5 exposure group and
593 PM2.5 exposure group+melatonin treatment group. Compared with the saline group,
594 the PM2.5 exposure group showed increased levels of MDA representing the level of
595 oxidation ($p<0.05$) and decreased levels of T-AOC ($p<0.001$) and GSH-Px ($p<0.01$)
596 representing antioxidant levels. The decrease of T-SOD was not obvious significantly
597 ($p<0.1$). PM2.5 exposure+melatonin group showed obviously decreased level of
598 MDA ($p<0.05$) and increased levels of T-AOC/T-SOD ($p<0.05$) and GSH-Px
599 ($p<0.01$). (B) Representative images of ROS stained by DHE fluorescence in
600 hypoglossal nucleus, cuneate nucleus, Botzinger complex and dorsal vagal complex.
601 (C) The bar graph representing quantified results of brain ROS respectively.

602 Compared with the saline group, the PM2.5 exposure group showed an increased
 603 production of ROS in the hypoglossal nucleus ($p<0.001$), cuneate nucleus ($p<0.001$),
 604 Botzinger complex ($p<0.05$), and DVC ($p<0.01$). Meanwhile, ROS production in
 605 PM2.5 exposure+melatonin group was decreased in Botzinger complex ($p<0.05$),
 606 cuneate nucleus ($p<0.05$), hypoglossal nucleus ($p<0.01$) and DVC ($p<0.01$). The
 607 values are presented as the means \pm S.E.M. * $p<0.05$, ** $p<0.01$, *** $p<0.001$, and
 608 # $p>0.05$, independent-samples T-test. n=4-6 per group. cc: central canal. $\times 200$



609

610

611 Fig 6.

612 Levels of TRPM2 in medulla oblongata of saline control group, PM2.5 exposure
613 group and PM2.5 exposure group+melatonin treatment group. (A) Representative
614 images of TRPM2 expression (red) in the Botzinger complex and dorsal vagal
615 complex. Nuclei were counterstained with DAPI (blue). (B) The bar graphs
616 representing quantified results of cell counting. Compared with the saline group, the
617 PM2.5 exposure group showed an increased expression of TRPM2 in the DVC and
618 Botzinger complex ($p<0.01$). Melatonin treatment decreased the expression of
619 TRPM2 ($p<0.05$) (Fig. 5A 5B). (C) Western blot showing protein level of TRPM2 in
620 medulla oblongata. (D) The bar graphs representing quantified results of TRPM2. The
621 protein level of TRPM2 in PM2.5 exposure group was higher than the saline group
622 ($p<0.001$) and PM2.5 exposure+melatonin group showed decreased protein level in
623 the DVC ($p<0.01$) and Botzinger complex ($p<0.05$). The values are presented as the
624 means \pm S.E.M. * $p<0.05$, ** $p<0.01$, and *** $p<0.001$, independent-samples T-test.
625 (n=6). cc: central canal. $\times 200$

